

Time-Resolved Fluorescence Study of Conformational Dynamics in Opioid Peptides

Greg S. Harms, William L. Freund, and Carey K. Johnson*

Department of Chemistry, University of Kansas, Lawrence, Kansas 66045

Received: January 8, 1998; In Final Form: April 6, 1998

Rotational correlation times have been determined from fluorescence anisotropy decays of the tyrosyl residue in the opioid pentapeptides DPDPE (Tyr-D-Pen-Gly-Phe-D-Pen), DPDPE(SH)₂, and [Leu⁵]-enkephalin, revealing internal peptide motions. Fluorescence decays were measured by time-correlated single-photon counting. For all three peptides, the fluorescence emission is characterized by three-exponential intensity decays with amplitudes that are consistent with ground-state populations of rotamers of the tyrosyl side chain. Rotational correlation times in water determined from single-exponential fits are 80–130 ps, in good agreement with molecular dynamics simulations [Wang, Y.; Kuczera, K. *J. Phys. Chem.* **1996**, *100*, 2555–2563]. Internal peptide motions were studied by measurement of the rotational correlation times in solutions of 50% propylene glycol in water over the temperature range from 258 to 313 K. Two distinct temperature regions were observed. In the low-temperature regime the thermal viscosity coefficient for each peptide is approximately 0.07 K⁻¹, the same as for free tyrosine. Hence, in this temperature regime the rotational friction is imposed by the solvent alone, consistent with rigid-body rotational motion. At higher temperatures an additional source of reorientational motion is revealed by an apparent change in the thermal viscosity coefficient. The viscosity coefficient in the high-temperature regime is characteristic of the peptide and not just the solvent, indicating the influence of internal dynamics. Double-exponential fits yielded further evidence of internal tyrosyl reorientational motions, which make increasingly large relative contributions at higher temperatures.

Introduction

Ever since the discovery of multiple opioid receptors with varying structural and conformational binding requirements^{1,2} (reviewed in refs 3 and 4), there has been a great interest in developing opioid analogues with the goal of exploring favorable binding configurations and eventually developing new analgesic drugs.^{5,6} One group of opioid receptor agonists of particular interest is the group of small peptides known as enkephalins.⁷ These compounds, found in the central nervous system, bind to the δ -opioid receptor in the brain and deaden pain sensations. Efforts to design peptides that are constrained to high-affinity conformations for their receptors have led to artificial peptides such as DPDPE (Tyr-D-Pen-Gly-Phe-D-Pen), a highly constrained synthetic enkephalin that shows superior binding to the δ -opioid receptor compared to its naturally occurring counterparts.⁵ DPDPE has been the focus of studies of peptide conformations by both NMR^{6,8,9} and computer simulations of peptide dynamics.^{10–12} However, time-resolved spectroscopic studies have not previously been reported.

Enkephalins are thought to form distinct conformations before binding to a receptor.^{6,13,14} In peptides, disulfide bonds often play a crucial role in the biological function of the molecule. In DPDPE, the disulfide bond is believed to stabilize a conformation that is biologically active. In this paper, we focus on the cyclic peptide with the disulfide bond (DPDPE) and its straight chain analogue DPDPE(SH)₂. Because the cyclic and the linear forms have different receptor binding affinities, it is important to understand how they differ conformationally and how these differences influence their dynamics.

Our approach is to relate fluorescence decays and fluorescence

depolarization to the conformational and reorientation dynamics in the opioid peptides. This approach probes fast conformational motions that occur on the subnanosecond time scale, overlapping the time regime that can be explored by molecular dynamics simulations. Internal motions and solvent-dependent rotational diffusion have been investigated previously in peptides and proteins by observing their temperature-dependent steady-state fluorescence polarization.^{15–17} Unlike tyrosine, which displayed a constant thermal coefficient of viscosity, tyrosyl containing peptides and proteins were found to exhibit two distinct regions with different viscosity dependencies in the temperature range from -40 to +20 °C. The low-temperature region is solvent limited, with a thermal viscosity coefficient that was nearly the same as that of free tyrosine for each of the peptides investigated. At higher temperatures, the thermal viscosity coefficient for peptides such as oxytocin and vasopressin was lower than that of free tyrosine. This suggests that conformational changes or internal motions in these peptides contribute to the fluorescence depolarization and might be detected in time-resolved experiments. During the past decade, both time-domain^{18,19} and frequency-domain^{20–22} techniques have been used to study tyrosyl fluorescence in peptides. Anisotropy decays attributable to local tyrosyl motions were detected in oxytocin, vasopressin, and [Leu⁵]-enkephalin.^{21,22}

Recent investigations in our laboratory have emphasized the use of anisotropy decays to identify the emitting species and to probe interactions with solvent.^{23,24} The purpose of this paper is to report the fluorescence and anisotropy decays of cyclic DPDPE, linear DPDPE(SH)₂, and [Leu⁵]-enkephalin (LE) investigated by time-correlated single-photon counting (TCSPC). We show that the peptide fluorescence intensity decays can be explained by the rotamer model for tyrosine. We also report fluorescence anisotropy decays with contributions from both

* To whom correspondence should be addressed. E-mail: cjohnson@eureka.chem.ukans.edu.

internal tyrosyl motions and rotational diffusion of the peptides as a whole. The temperature-dependent rotational behavior of the peptides is analyzed by a time-resolved analogue of the steady-state temperature dependence observed by Weber et al.^{16,17} We conclude that the thermal viscosity effect can be related to the loss of internal motion of the peptide as temperature decreases.

Materials and Methods

The fluorescence excitation pulse was provided by a cavity-dumped rhodamine-590 dye laser, and the resulting fluorescence signal was processed by TCSPC. The laser system and TCSPC instrumentation have been described in detail elsewhere.²³ Isotropic intensity decays (I_{MA}) were measured by setting the emission polarizer to the magic angle, 54.7° from vertical. Fluorescence depolarization measurements were obtained by collection of fluorescence polarized parallel ($I_{||}$) and perpendicular (I_{\perp}) to the excitation polarization. Fluorescence and anisotropy decays were analyzed by nonlinear least-squares fitting. In most cases, optimized fitting parameters for the population decay function obtained from fits to $I_{||}$ and I_{\perp} were nearly identical to those obtained from magic-angle fits. For the few exceptions, fits to $I_{||}(t)$ and $I_{\perp}(t)$ were obtained with the population-decay parameters fixed to values previously obtained from magic-angle measurements. In some cases the initial anisotropy value $r(0)$ for single-exponential rotational fits was fixed to an independently determined value. For double-exponential fits to anisotropy decays the initial anisotropy values were floated.

Samples. LE was purchased from Sigma. Linear DPDPE-(SH)₂ was a generous gift from Prof. Henry Mosberg. Cyclic DPDPE was provided by the National Institute on Drug Abuse (NIDA) or (for initial experiments) purchased from Sigma. All samples were HPLC pure and were checked by standard methods. Samples were dissolved in Nanopure water adjusted to pH 7 or in 10-mM pH 7 phosphate buffer. Sample concentrations were 20–80 μ M. For the temperature-dependent studies, samples were dissolved in 50% propylene glycol-water at the same concentration as aqueous samples. All samples were bubbled with a slow argon gas flow for 10 min to deoxygenate them prior to use.

Analysis of Temperature-Dependent Data. The thermal viscosity coefficient is extracted from the temperature dependence of the rotational correlation time, τ_{rot} , which was determined from a single-exponential fit to the anisotropy decay:

$$r(t) = r_0 \exp(-t/\tau_{rot}) \quad (1)$$

The temperature dependence of the rotational correlation time is given in hydrodynamic theory by the Stokes–Einstein–Debye (SED) equation:

$$\tau_{rot} = \frac{\eta V}{kT} F \quad (2)$$

where η is the viscosity, V is the molecular volume, k is the Boltzman constant, T is the absolute temperature, and F is a coupling factor ($F = 1$ for a sphere with sticking boundary conditions). The viscosity over a limited temperature range can be described by¹⁵

$$\eta = \eta_0 \exp[-b(T - T_0)] \quad (3)$$

where η_0 is the viscosity at temperature T_0 and b is the thermal coefficient of viscosity. From eqs 1 and 2, the temperature

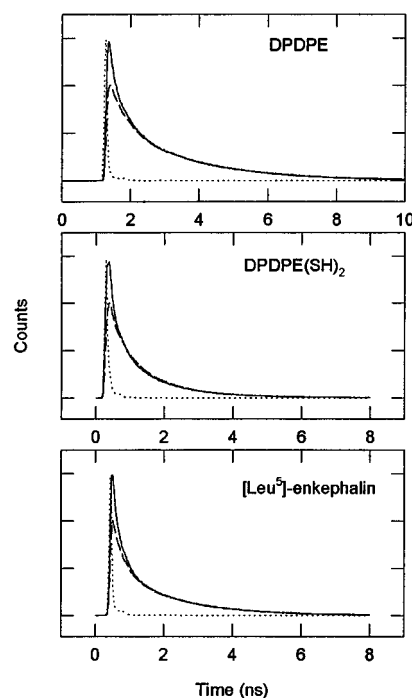


Figure 1. Fluorescence decays of cyclic DPDPE, linear DPDPE(SH)₂, and [Leu⁵]-enkephalin. In each case the upper decay curve is the decay of fluorescence polarized parallel to the excitation pulses ($I_{||}$) and the lower decay curve is the decay of fluorescence polarized perpendicular to the excitation pulses (I_{\perp}). The sharp peak is the instrument function. Fluorescence was excited at 287 nm and detected at 303 nm.

TABLE 1: Fluorescence and Anisotropy Decay Parameters for Opioid Peptides in Water ($\lambda_{ex} = 287$ nm; $\lambda_{em} = 305$ nm; Solvent Nanopure Water; pH 7)

| sample | a_i | τ_i (ns) | $\langle \tau \rangle^a$ (ns) | $r(0)$ | τ_{rot} (ps) | χ^2 |
|--------------------------------|-------|---------------|-------------------------------|--------|-------------------|----------|
| LE (20 °C) | 0.55 | 0.240 | 0.75 | 0.27 | 84 | 1.8 |
| | 0.35 | 1.500 | | | | |
| | 0.10 | 2.500 | | | | |
| DPDPE (25 °C) | 0.69 | 0.050 | 0.53 | 0.26 | 35 | 2.7 |
| | 0.20 | 0.812 | | | 233 | |
| | 0.11 | 3.024 | | | 126 | |
| DPDPE(SH) ₂ (25 °C) | 0.40 | 0.106 | 0.62 | 0.26 | 36 | 2.1 |
| | 0.33 | 0.319 | | | 300 | |
| | 0.27 | 1.743 | | | 124 | |
| | | | | | 35 | 1.1 |
| | | | | | 407 | |
| | | | | | | |

^a The average lifetime is given by $\langle \tau \rangle = \sum_i a_i \tau_i$.

dependence of the rotational correlation time is given by

$$\ln(\tau_{rot}/T) = -b(T - T_0) + \ln(\eta_0 VF/k) \quad (4)$$

Hence, a plot of $\ln(\tau_{rot}/T)$ versus temperature should yield the thermal viscosity coefficient in a manner analogous to the treatment of the steady-state anisotropy behavior employed by Weber and co-workers.¹⁵

Results

Fluorescence Intensity Decays. Figure 1 depicts the vertically and horizontally polarized emission decays of the tyrosyl residues in cyclic DPDPE, linear DPDPE(SH)₂, and LE in water at pH 7. The fluorescence and anisotropy decay fitting parameters are listed in Table 1. We find the fluorescence decays to require three lifetimes for a good fit. The multiexponential fluorescence decay is typical of tyrosyl moieties and

TABLE 2: Rotamer Populations of DPDPE (Cyclic)

| conformation | NMR populations (ref 8) | simulated populations (ref 11) | | preexponential factors ^a (this work) |
|--------------|-------------------------------|-----------------------------------|----------------|---|
| | | aq | saline (1.0 M) | |
| gauche(−) | 0.35 | 0.80 | 0.40 | 0.20 |
| trans | 0.62 | 0.13 | 0.60 | 0.69 |
| gauche(+) | 0.03 | 0.07 | 0.0 | 0.11 |

^a Assignment of the largest preexponential factor to the trans rotamer is based on comparison to the NMR results⁸ and molecular dynamics simulation¹² (see Discussion in text).

can be explained by the rotamer model.^{18,19,25,26} In this model, the three-exponential fluorescence decays of tyrosyl residues correspond to three conformers about the χ_1 bond having rotamer populations that correlate to steady-state populations measured by NMR. The different conformers have different fluorescence lifetimes depending on their proximity to quenching or electron withdrawing groups.

To justify our use of the rotamer model, we compared the preexponential factors for the fluorescence intensity decay to the rotamer populations for DPDPE determined by NMR⁸ and by computer simulation.¹¹ The three preexponential decay factors obtained from the analysis of the fluorescence decays are similar to the NMR-determined populations (see Table 2).

In the rotamer model^{18,25} the preexponential factors correspond to the ground-state populations in the gauche(−), trans, and gauche(+) orientations about the C_α – C_β bond for tyrosine. A comparison of the fluorescence preexponential factors for cyclic DPDPE (see Table 2) suggests that the largest rotamer population is associated with the shortest lifetime component. NMR analysis by Mosberg and co-workers⁸ correlates this component with the trans rotamer. Although one molecular dynamics simulation¹¹ assigns the largest population in water to the gauche(−) component, a longer (1 ns) molecular dynamics simulation¹² assigns the largest population to the trans conformer. Consistent with previous analyses of a number of peptides,^{19,23,25} this assignment identifies the shortest lifetime component with the trans rotamer.

The fluorescence decays of LE obtained by Lakowicz and co-workers²² with a 10 GHz frequency-domain instrument also contained three exponentials. The fitting amplitudes found for LE (Table 1) differ in certain details from the fits found by Lakowicz and co-workers. However, the average lifetime (0.91 ns) is close to that found by Lakowicz et al. (0.75 ns). The differences may be a result of the ambiguities inherent in multiple-parameter fits. For example, the short lifetime (0.24 ns) in our fit is roughly equal to the average (0.22 ns) of the two shorter lifetimes found by Lakowicz and co-workers,²² while the longer lifetime component found in ref 22 (1.51 ns) is roughly the average (1.72 ns) of the two longer lifetime components in our fit. We note that the average fluorescence lifetime is shorter for the cyclic form of DPDPE than for DPDPE(SH)₂ or LE, indicating enhanced fluorescence quenching in the cyclic form. Quenching of Tyr emission was previously observed by Schiller in cyclic [D-cys²,D-cys⁵] enkephalinamide relative to linear [Met⁵]–enkephalin.²⁷

Anisotropy Decays. In Table 1, rotational correlation times are given for fits performed with both one and two rotational components for DPDPE, DPDPE(SH)₂, and LE in water. The rotational correlation times determined from single-exponential anisotropy fits agree within experimental error with the rotational correlation times for the peptide as a whole (114–122 ps) found from molecular dynamics simulations of cyclic DPDPE and linear DPDPE(SH)₂ under the same conditions.¹² This close

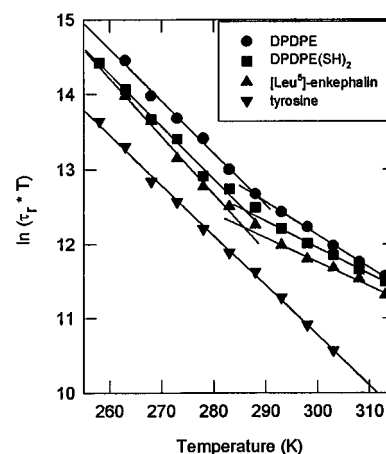


Figure 2. Plot of the natural log of $\tau_{\text{rot}} \cdot T$ as a function of temperature for DPDPE (●), DPDPE(SH)₂ (■), [Leu⁵]–enkephalin (▼), and free tyrosine (▲) in propylene glycol–water (1:1). The slopes of the solid lines yield the thermal viscosity coefficients. Values of the slopes obtained by linear regression and the temperature at which the low-temperature and high-temperature lines intersect are given in Table 4.

agreement is probably somewhat fortuitous, however, because the calculated rotational correlation time was obtained from the rotation of an axis system fixed to the peptide center of mass in the molecular dynamics simulation, whereas the measured rotational correlation time may include contributions from intramolecular conformational dynamics. Analysis of the measured anisotropy decays with two rotational correlation times results in significantly improved fits as judged by the value of χ^2 , suggesting that the experimental rotational correlation times include contributions from localized tyrosyl motions. (Incorporation of two rotational components does not significantly affect the fluorescence intensity decay fits.) In their analysis of anisotropy decays of LE by frequency-domain fluorometry, Lakowicz and co-workers also resolved two rotational components, 44 and 219 ps with amplitudes of $r_{0\text{fast}} \approx 0.22$ and $r_{0\text{slow}} \approx 0.10$.²² The results for LE in Table 1 correlate well with those values. The fast rotational component τ_{fast} for each peptide is close to the rotational time for free tyrosine in water.^{23,28} The longer rotational component τ_{slow} is most likely associated with rotational diffusion of the entire peptide.

Temperature Dependence. According to the SED equation (eq 2), rotational diffusion depends on temperature in two ways: explicitly through the factor T and implicitly through the temperature dependence of the viscosity η . Approximating the temperature dependence of η by eq 3, the temperature dependence of the rotational correlation time given by eq 4 predicts a linear relationship between the log of the product ηT and T . Figure 2 shows such plots for Tyr, DPDPE (cyclic), DPDPE(SH)₂ (linear), and LE in 50% propylene glycol–water. Like glycerol,¹⁵ propylene glycol provides a viscous environment for studies of peptide internal motions. The use of a viscous solvent environment allows more accurate measurements of the temperature dependence of rotational correlation times by extending the rotational decay over a larger fraction of the fluorescence time window. The rotational correlation times plotted in Figure 2 were determined from single-exponential fits to the anisotropy decays. Table 3 summarizes the data utilized in Figure 2.

The slopes of the plots in Figure 2 yield values of the thermal viscosity coefficient b in eq 4. Table 4 lists the thermal viscosity coefficients for tyrosine, DPDPE (cyclic), DPDPE(SH)₂ (linear), and LE from Figure 2. For free tyrosine, the plot is linear over the entire temperature range with a thermal viscosity coefficient

TABLE 3: Temperature Dependence of Anisotropy Decay Parameters of Opioid Peptides in Propylene Glycol–Water (1:1) ($\lambda_{\text{ex}} = 287 \text{ nm}$; $\lambda_{\text{em}} = 305 \text{ nm}$)

| temp (°C) | DPDPE ($r_0 = 0.26$) | | DPDPE(SH) ₂ ($r_0 = 0.26$) | | LE ($r_0 = 0.29$) | | tyrosine ($r_0 = 0.29$) | |
|--------------|---------------------------|----------|--|----------|------------------------|----------|------------------------------|----------|
| | τ_{rot} | χ^2 | τ_{rot} | χ^2 | τ_{rot} | χ^2 | τ_{rot} | χ^2 |
| −15 | | | 7087 | 2.6 | | | 3259 | 2.2 |
| −10 | 7171 | 3.0 | 4889 | 2.5 | 4482 | 2.6 | 2297 | 2.4 |
| −5 | 4398 | 2.7 | 3210 | 3.0 | 3130 | 2.7 | 1410 | 2.2 |
| 0 | 3198 | 2.7 | 2429 | 2.9 | 1882 | 2.9 | 1054 | 2.3 |
| 5 | 2397 | 2.8 | 1454 | 2.6 | 1264 | 2.9 | 721 | 1.8 |
| 10 | 1563 | 3.1 | 1203 | 2.7 | 948 | 2.8 | 515 | 2.7 |
| 15 | 1104 | 3.0 | 920 | 2.6 | 732 | 2.5 | 391 | 2.1 |
| 20 | 853 | 2.3 | 684 | 2.2 | 550 | 2.1 | 270 | 1.4 |
| 25 | 687 | 2.3 | 552 | 1.9 | 447 | 2.1 | 184 | 1.7 |
| 30 | 526 | 2.9 | 462 | 2.6 | 390 | 2.1 | 129 | 1.8 |
| 35 | 415 | 2.6 | 376 | 2.8 | 330 | 2.8 | | |
| 40 | 338 | 2.9 | 312 | 2.8 | 261 | 2.3 | | |

TABLE 4: Thermal Frictional Coefficients for Tyrosine and Opioid Peptides (Determined from Slopes in Figure 2; See Equation 4)

| sample | $b(\text{above } T_c)$ (K ^{−1}) | $b(\text{below } T_c)$ (K ^{−1}) | T_c |
|---------------------------------|--|--|-------|
| tyrosine | | 0.067 ± 0.003 | |
| LE | 0.033 ± 0.003 | 0.077 ± 0.006 | 288 |
| DPDPE (cyclic) | 0.044 ± 0.003 | 0.069 ± 0.003 | 288 |
| DPDPE(SH) ₂ (linear) | 0.036 ± 0.006 | 0.069 ± 0.005 | 286 |

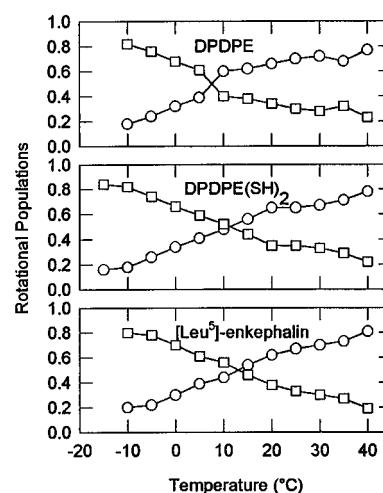
of 0.067 K^{-1} . The rotational motion can be attributed to rotational diffusion of the tyrosine molecule. Hence, the corresponding slope measures the thermal viscosity coefficient of the propylene glycol–water solvent. For the peptides, the rotational dynamics at low temperatures reveal nearly the same slope as for tyrosine, indicating that the friction experienced in this regime is characteristic of the solvent.¹⁵ At higher temperatures, however, a lower thermal viscosity coefficient is observed. The slopes in this region exhibit a viscosity coefficient characteristic of the peptide. A similar temperature dependence was observed previously by Weber and co-workers.^{16,17} The high-temperature viscosity coefficients determined from the slopes in Figure 2 are tabulated in Table 4. The temperature T_c at which linear fits to the low-temperature and high-temperature regions intersect is also listed in Table 4.

To examine whether the high-temperature reorientational dynamics contain internal motions, the anisotropy decays in propylene glycol were also fit with two rotational decay components:

$$r(t) = r_0[\alpha \exp(-t/\tau_{\text{fast}}) + \beta \exp(-t/\tau_{\text{slow}})] \quad (5)$$

where α and β are the relative amplitudes of the fast and slow correlation times. The resulting fitting parameters are presented in Table 5. In each case, incorporation of a second rotational component resulted in a significant improvement in the fit as shown by a comparison with the χ^2 values in Table 3. Figure 3 depicts the temperature dependence of the amplitudes α and β determined from the fits.

A word of caution is in order regarding the two-exponential fits to the anisotropy decays. The incorporation of a second exponential improves the statistical measure of goodness of fit, implying that the reorientational motions comprise two distinct processes. However, it does not follow that the two time constants determined in this way can be relied upon to provide accurate values for the rotational correlation times of the underlying reorientational motions. The reason lies in the uncertainties of multiple parameter fits, where variations in one

**Figure 3.** Temperature dependence of the amplitudes of the slow (\square) and fast (\circ) rotational times from double-exponential fits to the anisotropy decays of cyclic DPDPE, linear DPDPE(SH)₂, and [Leu⁵]-enkephalin in propylene glycol–water (1:1). The amplitudes were obtained from double-exponential fits to the anisotropy decays (see Table 5).**TABLE 5: Anisotropy Decay Parameters of Opioid Peptides. Temperature Dependence with Two Rotational Correlations ($\lambda_{\text{ex}} = 287 \text{ nm}$; $\lambda_{\text{em}} = 305 \text{ nm}$)**

| sample | temp (°C) | $r(0)$ | α | τ_{fast} (ps) | β | τ_{slow} (ps) | χ^2 |
|----------------|--------------|--------|----------|------------------------------|---------|------------------------------|----------|
| LE | −10 | 0.31 | 0.20 | 480 | 0.80 | 3700 | 1.3 |
| | −5 | 0.31 | 0.22 | 470 | 0.78 | 2990 | 1.8 |
| | 0 | 0.31 | 0.30 | 360 | 0.70 | 2600 | 1.8 |
| | 5 | 0.31 | 0.39 | 470 | 0.61 | 2500 | 1.6 |
| | 10 | 0.31 | 0.44 | 340 | 0.56 | 1900 | 1.5 |
| | 15 | 0.31 | 0.54 | 360 | 0.46 | 1850 | 1.5 |
| | 20 | 0.31 | 0.62 | 210 | 0.38 | 1900 | 1.1 |
| | 25 | 0.31 | 0.67 | 380 | 0.33 | 2200 | 1.4 |
| | 30 | 0.31 | 0.70 | 320 | 0.30 | 2300 | 1.2 |
| | 35 | 0.31 | 0.73 | 250 | 0.27 | 2100 | 1.3 |
| | 40 | 0.31 | 0.81 | 290 | 0.19 | 2200 | 1.2 |
| | −15 | 0.30 | 0.16 | 300 | 0.84 | 3400 | 1.8 |
| | −10 | 0.30 | 0.18 | 340 | 0.82 | 3300 | 1.4 |
| | −5 | 0.30 | 0.26 | 400 | 0.74 | 3800 | 1.8 |
| | 0 | 0.30 | 0.34 | 410 | 0.66 | 2900 | 1.5 |
| | 5 | 0.30 | 0.41 | 390 | 0.59 | 2900 | 1.4 |
| DPDPE (linear) | 10 | 0.30 | 0.48 | 380 | 0.52 | 3300 | 1.6 |
| | 15 | 0.30 | 0.56 | 410 | 0.44 | 2950 | 2.2 |
| | 20 | 0.30 | 0.65 | 400 | 0.35 | 2800 | 1.2 |
| | 25 | 0.30 | 0.65 | 380 | 0.35 | 2800 | 1.7 |
| | 30 | 0.30 | 0.67 | 380 | 0.33 | 2900 | 1.7 |
| | 35 | 0.30 | 0.71 | 330 | 0.29 | 2300 | 1.9 |
| | 40 | 0.30 | 0.78 | 270 | 0.22 | 2500 | 2.1 |
| | −10 | 0.30 | 0.18 | 340 | 0.82 | 3600 | 2.1 |
| | −5 | 0.30 | 0.24 | 350 | 0.76 | 3300 | 2.2 |
| | 0 | 0.30 | 0.32 | 380 | 0.68 | 3200 | 1.7 |
| | 5 | 0.30 | 0.39 | 420 | 0.61 | 3100 | 1.8 |
| | 10 | 0.30 | 0.60 | 310 | 0.40 | 3100 | 2.1 |
| | 15 | 0.30 | 0.62 | 290 | 0.38 | 3250 | 1.9 |
| | 20 | 0.30 | 0.66 | 350 | 0.34 | 3400 | 2.2 |
| | 25 | 0.30 | 0.70 | 340 | 0.30 | 2500 | 2.1 |
| | 30 | 0.30 | 0.72 | 260 | 0.28 | 1800 | 1.7 |
| DPDPE (cyclic) | 35 | 0.30 | 0.68 | 290 | 0.32 | 1500 | 1.5 |
| | 40 | 0.30 | 0.77 | 350 | 0.23 | 1600 | 2.0 |

fitting parameter can often be compensated to a large degree by shifts in other parameters, resulting in a fit that is nearly as “good”. Hence, we do not expect that the numerical values of the two correlation times determined by two-exponential fits are necessarily meaningful. Rather, these fits show that there are in fact two processes, one fast and the other slow, contributing to the dynamics. It is reasonable to conclude from

the fits in Table 5 that the slow process dominates the reorientational dynamics at low temperatures and the fast process dominates the dynamics at high temperatures. For quantitative examination of the temperature dependence of the anisotropy decay, we have chosen to analyze the rotational correlation time determined by single-exponential fits.

Discussion

The fluorescence anisotropy decays report the reorientational dynamics of the tyrosyl residues. Reorientational motions may include both overall rotational motion of the peptide (rotational diffusion) and intramolecular motions. The latter could be associated with floppy conformational modes of the peptide backbone or with localized motions of the tyrosyl side chains. Significant internal motions in DPDPE have been detected in molecular dynamics simulations.¹²

From the double-exponential fits to the anisotropy decays, it is possible to draw general conclusions about the nature of the contributing dynamics. The long component, on the order of 200–400 ps in water, can be attributed to rotational diffusion of the peptide as a whole. This conclusion is based principally on the time scale of the motion, which is 6–10 times the 38 ps rotational diffusion time of free tyrosine.^{23,28} The fast rotational contribution can in turn be assigned to intramolecular motions. The fast time scale of this component, which is comparable to the rotational diffusion time of free tyrosine, suggests a localized motion of the tyrosine side chain itself. The large amplitude associated with this component demonstrates significant motion of the tyrosyl side chain in the peptide.

In propylene glycol–water both rotational components are slowed considerably by the increased viscosity of the solvent. The double-exponential fits again reveal two contributing motions. However, it is more reliable for quantitative comparisons to characterize the rotational dynamics by a single rotational correlation time (Table 3), which represents the rotational dynamics with a minimum number of parameters.

The temperature dependence of the rotational correlation times is shown in Figure 2. A comparison of the rotational dynamics of the cyclic and linear forms of DPDPE (see Table 3 and Figure 2) shows that the rotational correlation time of the cyclic peptide is longer than that of linear DPDPE(SH)₂ in propylene glycol–water (see Figure 2). Because the peptides DPDPE and DPDPE(SH)₂ are expected to have similar size and shape,¹² their rotational diffusion times are likely to be roughly equal. This suggests that the shorter rotational correlation time for DPDPE(SH)₂ may result from increased flexibility of the peptide, which would contribute a faster component to the overall rotational correlation time. This conclusion is consistent with increased flexibility of the linear form found in molecular dynamics simulations¹² and may be related to the enhanced permeability of linear DPDPE(SH)₂ through membranes.^{9,29}

The fact that the reorientational dynamics of the three peptides fall into two regimes, a low-temperature and a high-temperature regime, raises the interesting question: what is the source of the transition from one regime to another? At low temperatures, the reorientational motions of each of the peptides is governed by the friction of the surrounding propylene glycol–water solvent. This can be seen by comparison of the slopes in Figure 2 with the slope for free tyrosine. In this regime the ratio of the peptide rotational correlation times to the rotational correlation time of tyrosine is essentially constant with values of roughly 1.9 for LE, 2.2 for DPDPE(SH)₂, and 3.0 for DPDPE, as shown in Figure 4. These values are consistent with the ratios observed for the rotational correlation times determined in water

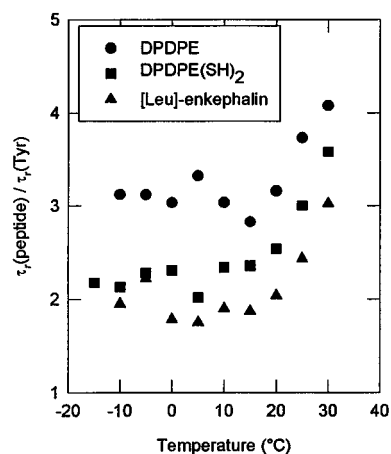


Figure 4. Ratio of the rotational correlation times of peptides to the rotational correlation time of free tyrosine for DPDPE (●), DPDPE(SH)₂ (■), and [Leu⁵]-enkephalin (▼) in propylene glycol–water (1:1). The rotational correlation times were obtained from single-exponential fits to the anisotropy decays (see Table 3).

(Table 1). The simplest explanation is that the reorientational motion in this regime is dominated by overall rotational diffusion of the peptide as a whole. According to the SED equation (eq 2), the ratio of correlation times is determined by the ratio of the volume of the peptide to the volume of tyrosine and the ratio of coupling coefficients. In the low-temperature regime where the ratio of correlation times is constant, these ratios do not change noticeably with temperature.

In the high-temperature regime, the tyrosyl reorientations in the peptide are no longer controlled solely by the solvent. As temperature increases, the ratio of the peptide rotational correlation time to that of free tyrosine becomes increasingly large (see Figure 4). This is also reflected in the slope changes in Figure 2. In the high-temperature regime, the rotational correlation times no longer track the rotational diffusion of free tyrosine. Similar behavior was observed over a decade ago by Weber and co-workers^{16,17} in steady-state fluorescence measurements. These workers proposed a chemical equilibrium model in which a strongly solvated state characteristic of lower temperatures is in equilibrium with a less solvated state characteristic of higher temperatures. The sharpness of the transition from the low- to high-temperature regimes is a measure of the enthalpy increase ΔH .

With time-resolved detection of the anisotropy decay, further information about the nature of the reorientational dynamics in the high-temperature regime can now be garnered from the time dependence of the anisotropy decays. In the model proposed by Weber and co-workers,¹⁶ tyrosyl reorientations are characterized by a single reorientational component. These reorientations are controlled by the friction of the solvent at low temperatures. At higher temperatures, changes in the peptide shape or peptide–solvent coupling were suggested to engender a reduced interaction with the solvent resulting, for example, from disruptions of hydrogen bonding interactions with the solvent.¹⁶

The time-resolved measurements lead us to favor a different model of reorientational dynamics, one that is suggested by the fits with two rotational decay times. The improvement in the fits with second correlation times as measured by χ^2 (Table 5) is strong evidence that two underlying dynamical processes contribute to the reorientational motions in these peptides. What are these two processes? A logical candidate for the slow reorientational time is rotational diffusion of the peptide as a whole. The predominance of rotational diffusion at low temperature is supported by the two-exponential fits (Table 5),

in which the amplitude of the long rotational component becomes large at low temperature.

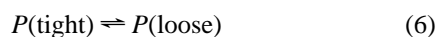
The short decay is roughly a factor of 10 faster than the long decay component (see Table 5). As Table 5 shows, this time constant does not seem to depend strongly on temperature for any of the three peptides. However, the relative contribution of the short component (α in eq 5) grows with increasing temperature. This suggests that the short decay component is restricted not so much by frictional resistance of the solvent as by limitations on the available amplitude of motion. It seems reasonable to suppose that this component reflects a rather localized reorientational motion, perhaps of the tyrosyl side chain itself.

This shift in the contributions of slow and fast rotational times is the underlying cause of the behavior of the viscosity-dependent slopes in Figure 2. At low temperature, internal motions are frozen out, leaving rotational diffusion as the source of reorientational motion. As the temperature approaches T_c , internal motions contribute more and more to the anisotropy decay. At higher temperatures, the greater contribution of the fast component is associated with a lower thermal viscosity coefficient than for free tyrosine. It may seem odd that the increasing contributions from the *fast* rotational component would lead to a less precipitous decline with temperature in the rotational correlation times as determined in single-exponential fits. This occurs because the fast rotational time is not strongly temperature dependent. Hence, the rate of internal motions does not accelerate as rapidly as the rate of rotational diffusion.

The fast rotational motion can be viewed as reorientational motion restricted in amplitude. The rotational *rate* is not strongly temperature dependent because the reorientation is not strongly coupled to the solvent. The *amplitude* of the anisotropy decay associated with the fast rotation is, however, temperature dependent. This could arise from the formation of a "looser" conformation at high temperatures with an increased free volume available for the fast decay component. The fact that the temperature coefficient for this increase in amplitude is weaker than the temperature coefficient for the solvent viscosity most likely reflects the nature of the forces involved. The solvent viscosity decreases with increasing temperature due to the disruption of relatively strong hydrogen bonding interactions, whereas the transition to a higher amplitude of the fast decay involves weaker van der Waals forces. One candidate for these forces is intramolecular tyrosine-phenylalanine interactions.

To examine the validity of this model with contributions from localized Tyr dynamics growing in at higher temperatures, we have attempted to model the observed behavior quantitatively. As pointed out over a decade ago by Weber and co-workers,¹⁶ however, a detailed explanation of the contributions to the reorientational dynamics will probably require extensive molecular dynamics simulations. Nevertheless, it is useful to show that the proposed model can explain the observed rotational correlation times.

We consider a conformational transition in the peptide that leads from a low-temperature conformation where localized motion of the tyrosyl residue is restricted to a high-temperature conformation with greater freedom for localized tyrosyl motion:



The measured rotational correlation time (as given by single-exponential fits to the anisotropy decay) is taken to be an average of two contributions, τ_1 and τ_2 .³⁰

$$\tau_{\text{rot.}} = f_1 \tau_1 + f_2 \tau_2 \quad (7)$$

where τ_1 is the contribution from $P(\text{tight})$ and τ_2 is the contribution from $P(\text{loose})$. The weights f_1 and f_2 are given by the relative populations of the two conformations, $P(\text{tight})$ and $P(\text{loose})$, determined by the equilibrium constant for eq 6. Anisotropy decay including localized motion is described by

$$r(t) = r(0)[\alpha \exp(-t/\tau_{\text{loc.}}) + (1 - \alpha) \exp(-t/\tau_{\text{rot.}})] \quad (8)$$

where $\tau_{\text{loc.}}$ is the correlation time for localized motion and $\tau_{\text{rot.}}$ is the rotational diffusion time constant. The relative contributions of overall rotational diffusion and internal Tyr motion are determined by the degree of restriction of the localized motion, given by the parameter α in eq 5. The contribution from rotational diffusion is expected to dominate the low-temperature conformation, while the contribution from local tyrosyl motion is expected to dominate the high-temperature conformation. The rotational diffusion time $\tau_{\text{rot.}}$ can be described by

$$\tau_{\text{rot.}} = \tau_0 \frac{T_0}{T} \exp[-b_{\text{rot.}}(T - T_0)] \quad (9)$$

Similarly, for purposes of model calculations, the local tyrosine reorientation $\tau_{\text{loc.}}$ can be represented by

$$\tau_{\text{loc.}} = A \frac{T_0}{T} \exp[-b_{\text{loc.}}(T - T_0)] \quad (10)$$

where A is a constant setting the scale of the fast reorientational motions and $b_{\text{loc.}}$ is expected to be much smaller than $b_{\text{rot.}}$, indicating the weaker coupling of the local motion to the solvent friction.

This model is capable of explaining the observed temperature dependence. Figure 5 shows fits to the temperature dependence of the rotational correlation times of cyclic DPDPE, DPDPE-(SH)₂, and LE in propylene glycol-water, with α set to 0 for the low-temperature conformation $P(\text{tight})$ and to the value 0.9 for $P(\text{loose})$. (See figure caption for values of the fitting parameters.) The purpose of these fits is to demonstrate the consistency of the model with the observed temperature dependence and not to extract values for the parameters in the model. Specifically, the appearance of the plots of $\ln(\tau_{\text{rot.}}T)$ as a function of viscosity (Figure 2), with linear low- and high-temperature regions, is explained by this model. The high-temperature slope b given in Table 4 is a composite effect of both the enthalpy change ΔH for eq 6, leading to increased contributions from localized tyrosyl motions, and the temperature factor $b_{\text{loc.}}$ of the friction that characterizes these localized motions.

Conclusions

The rotational correlation times of DPDPE and related peptides have been measured to examine their reorientational dynamics. The measured reorientational correlation time in water is consistent with values calculated from the molecular dynamics simulations of Wang and Kuczera.¹² In a more viscous environment, the temperature dependence of the rotational correlation time reveals two regions that can be characterized by different thermal friction coefficients, in a manner analogous to the analysis of steady-state anisotropy measurements.^{16,17} We suggest that the faster rotational relaxation in linear DPDPE-(SH)₂, even in the low-temperature regime, is associated with its higher flexibility relative to DPDPE, consistent with previous observations.^{9,12} The temperature-

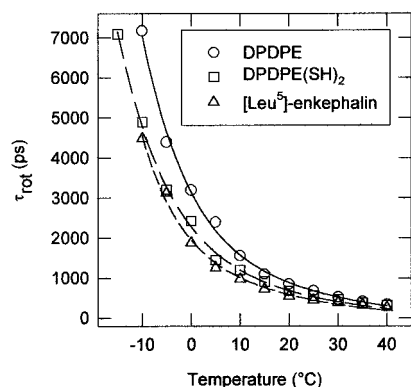


Figure 5. Examples of fits of the rotational correlation times of cyclic DPDPE (○), linear DPDPE(SH)₂ (□), and [Leu⁵]-enkephalin (△) in propylene glycol–water (1:1) to a model with reorientational contributions from both overall rotational diffusion and from local motions of the Tyr side chain (see text for details). The lines through the data are plots of the model in eqs 6–9 with the following parameter values. DPDPE: $\Delta H = 27 \text{ kJ mol}^{-1}$; $\Delta S = 103 \text{ J K}^{-1} \text{ mol}^{-1}$; $b_{\text{rot}} = 0.068 \text{ K}^{-1}$; $b_{\text{loc}} = 0.0029 \text{ K}^{-1}$; $\tau_0 = 7440 \text{ ps}$; $A = 1140 \text{ ps}$. DPDPE(SH)₂: $\Delta H = 22 \text{ kJ mol}^{-1}$; $\Delta S = 88 \text{ J K}^{-1} \text{ mol}^{-1}$; $b_{\text{rot}} = 0.066 \text{ K}^{-1}$; $b_{\text{loc}} = 0.00074 \text{ K}^{-1}$; $\tau_0 = 4956 \text{ ps}$; $A = 953 \text{ ps}$. LE: $\Delta H = 41 \text{ kJ mol}^{-1}$; $\Delta S = 160 \text{ J K}^{-1} \text{ mol}^{-1}$; $b_{\text{rot}} = 0.071 \text{ K}^{-1}$; $b_{\text{loc}} = 0.0050 \text{ K}^{-1}$; $\tau_s = 4784 \text{ ps}$; $\tau_f = 1143 \text{ ps}$.

dependent behavior of the opioid peptides studied here can be explained by a loss of internal motions at low temperatures. The time-resolved anisotropy decays reveal fast and slow reorientational contributions to the rotational correlation times. The fast reorientational component can be associated with internal motion of the tyrosyl group and the slow component with rotational diffusion. This behavior can be explained by a transition to a peptide conformation allowing more flexibility of the tyrosyl fluorophore. The fact that the rotational correlation times of all three peptides (LE, DPDPE, DPDPE(SH)₂) show a similar temperature dependence suggests that an intrinsic change occurs in the dynamics at high temperature.

Acknowledgment. We thank Prof. Henry Mosberg and Prof. Krzysztof Kucera for their helpful comments. We wish to thank Prof. Henry Mosberg for a gift of DPDPE(SH)₂ and Dr. Kevin Gormley and the National Institute on Drug Abuse for DPDPE. We are grateful to Prof. Graham Fleming and to Dr. Gary Holtom for sharing their TCSPC fitting programs with us. W.L.F. acknowledges support by a University of Kansas undergraduate research award. This work was supported by NSF (EPSCoR Grant No. 9550487).

References and Notes

- (1) Lord, J. A. H.; Waterfield, A. A.; Hughes, J.; Kosterlitz, H. W. *Nature* **1977**, 267, 495.
- (2) Wolozin, B. L.; Pasternak, G. W. *Proc. Natl. Acad. Sci. U.S.A.* **1981**, 78, 6181.
- (3) Schiller, P. W. In *Opioid Peptides: Biology, Chemistry, Genetics*; Udenfriend, S., Meienhofer, J., Eds.; Academic Press: New York, 1984; Vol. 6, p 219.
- (4) Hruby, V. J.; Patel, D. Structure–Function Studies of Peptide Hormones: An Overview. In *Peptides: Synthesis, Structures, and Applications*; Gutte, B., Ed.; Academic Press: San Diego, 1995; p 247.
- (5) Mosberg, H. I.; Hurst, R.; Hruby, V. J.; Gee, K.; Yamamura, H. I.; Galligan, J. J.; Burks, T. F. *Proc. Natl. Acad. Sci. U.S.A.* **1983**, 80, 5871.
- (6) Hruby, V. J.; Kao, L.-F.; Pettitt, B. M.; Karplus, M. *J. Am. Chem. Soc.* **1988**, 110, 3351.
- (7) Hughes, J.; Smith, T. W.; Kosterlitz, H. W.; Fothergill, L. A.; Morgan, B. A.; Morris, H. R. *Nature* **1975**, 258, 577.
- (8) Mosberg, H. I.; Sobczyk-Kojiro, K.; Subramanian, P.; Crippen, G. M.; Ramalingam, K.; Woodard, R. W. *J. Am. Chem. Soc.* **1990**, 112, 822.
- (9) Matsunaga, T. O.; Collins, N.; Ramaswami, V.; Yamamura, H. I.; O'Brien, D. F.; Hruby, V. J. *Biochemistry* **1993**, 32, 13180.
- (10) Smith, P. E.; Dang, L. X.; Pettitt, B. M. *J. Am. Chem. Soc.* **1991**, 113, 67.
- (11) Smith, P. E.; Pettitt, B. M. *Biopolymers* **1992**, 32, 1623.
- (12) Wang, Y.; Kucera, K. *J. Phys. Chem.* **1996**, 100, 2555.
- (13) Nikiforovich, G. V.; Hruby, V. J.; Prakash, O.; Gehrig, C. A. *Biopolymers* **1991**, 31, 941.
- (14) Lomize, A. L.; Pogozheva, I. D.; Mosberg, H. I. *Biopolymers* **1996**, 38, 221.
- (15) Weber, G.; Scarlata, S.; Rholam, M. *Biochemistry* **1984**, 23, 6785.
- (16) Scarlata, S.; Rholam, M.; Weber, G. *Biochemistry* **1984**, 23, 6789.
- (17) Rholam, M.; Scarlata, S.; Weber, G. *Biochemistry* **1984**, 23, 6793.
- (18) Gauduchon, P.; Wahl, P. *Biophys. Chem.* **1978**, 8, 87.
- (19) Ross, J. B. A.; Laws, W. R.; Buku, A.; Sutherland, J. C.; Wyssbrod, H. R. *Biochemistry* **1986**, 25, 608.
- (20) Lakowicz, J. R.; Laczko, G.; Gryczynski, I. *Biochemistry* **1987**, 26, 82.
- (21) Gryczynski, I.; Szmancinski, H.; Laczko, G.; Wicz, W.; Johnson, M. L.; Kusba, J.; Lakowicz, J. R. *J. Fluoresc.* **1991**, 1, 163.
- (22) Lakowicz, J. R.; Gryczynski, I.; Laczko, G.; Wicz, W. *Biophys. Chem.* **1993**, 47, 33.
- (23) Harms, G. S.; Pauls, S. W.; Hedstrom, J. F.; Johnson, C. K. *J. Fluoresc.* **1997**, 7, 273.
- (24) Harms, G. S.; Pauls, S. W.; Hedstrom, J. F.; Johnson, C. K. *J. Fluoresc.* **1997**, 7, 283.
- (25) Laws, W. R.; Ross, J. B. A.; Wyssbrod, H. R.; Beechem, J. M.; Brand, L.; Sutherland, J. C. *Biochemistry* **1986**, 25, 599–607.
- (26) Ross, J. B. A.; Laws, W. R.; Rousslang, K. W.; Wyssbrod, H. R. Tyrosine Fluorescence and Phosphorescence from Proteins and Polypeptides. In *Topics in Fluorescence Spectroscopy*; Lakowicz, J. R., Ed.; Plenum Press: New York, 1992; Vol. 3, pp 1–63.
- (27) Schiller, P. W. *Biochem. Biophys. Res. Commun.* **1983**, 114, 268.
- (28) Lakowicz, J. R.; Maliwal, B. P. *J. Biol. Chem.* **1983**, 258, 4794.
- (29) Ramaswami, V.; Haaseth, R. C.; Matsunaga, T. O.; Hruby, V. J.; O'Brien, D. F. *Biochim. Biophys. Acta* **1992**, 1109, 195.
- (30) Model calculations show that this average represents reasonably well the value obtained by a least-squares fit to a double-exponential decay over the range of parameters fit here.